



# A comparative EPR study of high- and low-spin $Mn_6$ single-molecule magnets

Saiti Datta<sup>a</sup>, Erica Bolin<sup>a</sup>, Ross Inglis<sup>b</sup>, Constantinos J. Milios<sup>b</sup>, Euan K. Brechin<sup>b</sup>, Stephen Hill<sup>a,c,\*</sup>

<sup>a</sup> Department of Physics, University of Florida, P.O. Box 118440, Gainesville, FL 32611, USA

<sup>b</sup> School of Chemistry, The University of Edinburgh, EH9 3JJ, UK

<sup>c</sup> National High Magnetic Field Laboratory and Department of Physics, Florida State University, Tallahassee, FL 32310, USA

## ARTICLE INFO

### Article history:

Available online 21 January 2009

### Keywords:

Single-molecule magnet  
Electron paramagnetic resonance  
Spin-orbit interaction  
Manganese  
Magnetic anisotropy

## ABSTRACT

We report detailed numerical and spectroscopic studies of two complexes from a family of recently discovered  $Mn_6^{III}$  single-molecule magnets (SMMs) with large barriers to magnetization reversal. These complexes consist of a pair of  $Mn_3^{III}$  triangles with a ferromagnetic interaction between the triangles. Recent studies have shown that the exchange interactions within the triangular  $Mn_3^{III}$  units can be switched from antiferromagnetic to ferromagnetic, resulting in a switching of the spin from  $S = 4$  to 12. This strategy to “increase  $S$ ” has resulted in the highest magnetic energy barrier and blocking temperature for any known SMM to date. Extensive frequency, temperature and field-orientation dependent single-crystal high-frequency electron paramagnetic resonance measurements have been performed to determine the spin-Hamiltonian parameters associated with the lowest-lying spin multiplet for each complex. We compare the experimental findings with numerical calculations, where the total anisotropy for a complex is determined in terms of single-ion anisotropies using both projection operator techniques and exact matrix diagonalization methods. In particular, we find that the product of the molecular anisotropy,  $D$ , and spin,  $S$ , does not change significantly upon switching from  $S = 4$  to 12, i.e.  $D$  goes down as  $S$  goes up. These studies provide important insights concerning strategies for designing SMMs with higher blocking temperatures, particularly for complexes containing manganese in its +3 oxidation state.

© 2008 Elsevier Ltd. All rights reserved.

## 1. Introduction

Magnetochemists have experimented with various polynuclear transition metal topologies since the first identification of the single-molecule magnet (SMM)  $Mn_{12}$ -acetate in 1993 [1]. SMMs are nanoscale molecules that can be magnetized at low temperatures such that they independently retain this magnetization without any long range interactions with neighboring molecules. Most of the SMMs synthesized to date have been based on manganese. There are two reasons for this: (1) the flexibility of manganese chemistry, particularly with regards to its multiple oxidation states, enables the engineering of large molecules with a significant unpaired electron count, i.e. a large magnetic moment or spin,  $S$ , thus far up to 83/2 [2,3]; and (2) octahedrally coordinated  $Mn^{III}$  atoms exhibit a tendency to undergo Jahn–Teller distortions which result in an appreciable molecular anisotropy,  $D$  [4]. It is these two ingredients, large  $S$  and  $D$ , that are the key to obtaining good SMMs: when combined, they give rise to a large barrier,  $U \approx |D|S^2$ , against magnetization relaxation.

\* Corresponding author. Address: National High Magnetic Field Laboratory and Department of Physics, Florida State University, Tallahassee, FL 32310, USA. Tel.: +1 352 392 5711.

E-mail address: [shill@magnet.fsu.edu](mailto:shill@magnet.fsu.edu) (S. Hill).

For a long time it was a common held belief that the  $Mn^{III}$ -based oxide-centered triangular topology could never lead to a SMM, because antiferromagnetic exchange interactions within the core would result in a low-spin ground state [5,6]. However, it has recently been demonstrated [7–9] that a relatively small ligand-induced structural distortion can switch the exchange between  $Mn^{III}$  atoms in a triangular unit from antiferromagnetic to ferromagnetic, leading to a high-spin ( $S = 6$ ) ground state. This was the first example of a Mn-based triangular SMM.

The  $Mn^{III}$  triangular units may also be used as ‘molecular bricks’ to build larger structures, leading to even larger spin values. In the recently discovered  $Mn_6$  family [10,11], two of these triangular units couple ferromagnetically giving a maximum possible spin ground state of  $S = 12$ . The exchange interactions within the triangle depend on the individual Mn–O–N–Mn torsion angles. Pairwise interactions (Mn···Mn) switch from antiferromagnetic to ferromagnetic when this angle exceeds a critical value ( $\sim 31^\circ$ ), leading to a change in spin from  $S = 4$  to 12 and a subsequent increase in the barrier height.

At first sight, the above strategy would appear to be excellent for obtaining SMMs with larger barriers, since  $U \propto S^2$ . However, one must also recognize that  $U$  depends on the molecular anisotropy parameter,  $D$ , which, in turn, depends on the projection of the individual single-ion anisotropies onto the total spin state,  $S$ , of the molecule. This projection is non-trivial, particularly for the

antiferromagnetic case, and must be taken into consideration when developing strategies for designing optimal SMMs. Indeed, it has recently been suggested that the barrier height may go as  $S^0$  [12,13] as the spin value increases, thus implying that  $U$  does not change in the process. In this paper, we show experimentally that  $U$  does increase, and that it goes roughly as  $S^1$  rather than  $S^2$  or  $S^0$ .

## 2. Experiment details

Multi-high-frequency electron paramagnetic resonance (EPR) measurements were performed on single-crystals of  $\text{Mn}_6^{\text{III}}\text{O}_2(\text{Me-sao})_6(\text{O}_2\text{CCPh}_3)_2(\text{EtOH})_4$  (**1**) and  $\text{Mn}_6^{\text{III}}\text{O}_2(\text{Et-sao})_6(\text{O}_2\text{CPh}(\text{Me})_2)_2(\text{EtOH})_6$  (**2**) at various frequencies from 50 to 350 GHz, and with dc fields applied along different crystallographic directions. Both complexes have monoclinic structures. However, magnetic data suggests complex **1** has a low spin ground state of  $S = 4$ , whereas complex **2** has a  $S = 12$  ground state with a uniaxial molecular anisotropy  $D = -0.43 \text{ cm}^{-1}$  [11]. Incidentally, it has been shown that **2** holds the record for the highest barrier for a SMM ( $U = 86.4 \text{ K}$  [10]). EPR signals from single-crystals were detected using a sensitive cavity-perturbation technique in combination with a Millimeter-wave Vector Network Analyzer (described elsewhere [14,15]).

## 3. Data and discussion

The magnetic axial directions of **1** and **2** were determined using the one- and two-axis rotation techniques, respectively (described elsewhere [9,16,17]). Extensive measurements at various temperatures and frequencies were then performed with the dc field applied parallel to the easy-axis to determine the zero-field splitting (ZFS) in the ground state, i.e. the parameters in the simple spin Hamiltonian,  $H = DS_z^2 + B_4^0 O_4^0 + g\mu_B \vec{B} \cdot \vec{S}$  (see [16] for an explanation of the operators/parameters).

Fig. 1 shows temperature-dependence spectra obtained at 331 GHz for complex **2** with the field applied approximately parallel to its easy-axis. A series of more-or-less evenly spaced resonances are seen (dips in transmission). As the temperature is reduced, intensity shifts from the higher field resonances to the lowest field transition. Based upon this observation, we can assign the peaks A1, A2, A3, A4, and A5 to the following EPR transitions:  $m_S = -12 \rightarrow -11$ ,  $-11 \rightarrow -10$ ,  $-10 \rightarrow -9$ ,  $-9 \rightarrow -8$ ,  $-8 \rightarrow -7$ , respectively, where  $m_S$  represents the spin projection along the easy ( $z$ -) axis of the crystal. Each of the peaks exhibits several fine structures on the high-field shoulders. This is quite a common observation

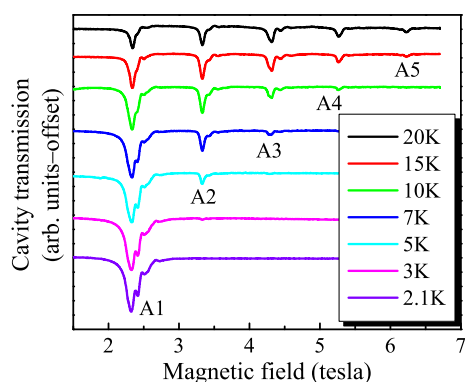


Fig. 1. Temperature dependence spectra obtained at 331 GHz for the easy-axis orientation for complex **2** ( $S = 12$ ). See text for explanation.

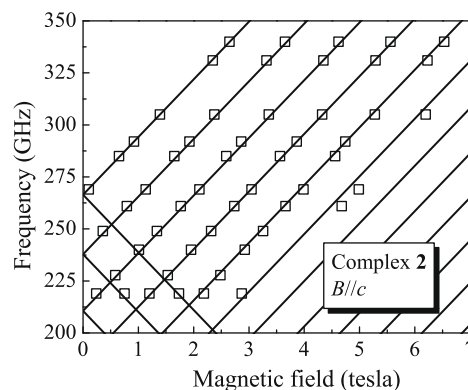


Fig. 2. Energy difference diagram constructed from frequency-dependent measurements for the easy-axis orientation for complex **2** at a temperature of 20 K. The solid lines are the simulations using the parameters given in the main text.

and likely signifies weak disorder in the crystal resulting in a distribution of microenvironments, i.e. a distribution in  $D$  [18].

Precise determination of the spin Hamiltonian parameters  $D$ ,  $B_4^0$  and  $g$  is made possible by recording EPR spectra at several high frequencies, as shown in Fig. 2 for this  $S = 12$  complex (**2**). Simulations for the easy-axis direction suggest that the system is best described with  $D = -0.360(5) \text{ cm}^{-1}$ ,  $B_4^0 = -5.7(5) \times 10^{-6} \text{ cm}^{-1}$  and  $g = 1.98(1)$ . One can obtain a fairly reliable estimate of the barrier from these parameters,  $U = 75 \text{ K}$ . This value is significantly lower than the one obtained from ac susceptibility measurements, though it remains the highest recorded value for any SMM. Similar discrepancies have been noted for many other SMMs, with ac susceptibility measurements consistently giving larger values for the 'effective' barrier in comparison to spectroscopic measurements [19].

Measurements performed on the  $S = 4$  complex (**1**) give the following spin Hamiltonian parameters:  $D = -1.272 \text{ cm}^{-1}$  and  $B_4^0 = +1.3(3) \times 10^{-4} \text{ cm}^{-1}$ ;  $g$  was not well determined because the field was only approximately aligned with the easy axis (within  $15^\circ$ ). Fig. 3 shows the best simulation of the frequency dependent data for complex **1**. In addition to the main peaks corresponding to the  $S = 4$  state (black squares), a weaker series of peaks is observed, as indicated in the figure by black circles and the dashed line. We note that it is not possible to simulate both sets of peaks simultaneously, even for spin values different from  $S = 4$ . We thus conclude that the extra peaks result from a low-lying excited state,

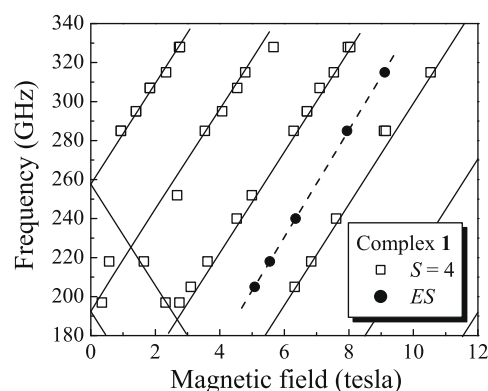


Fig. 3. Energy difference diagram constructed from frequency-dependent measurements for the field close to the easy-axis direction for complex **1**. The solid lines are the simulations using the parameters given in the main text for  $S = 4$ . The round data points and the dashed line correspond to excitations within a presumed low-lying excited state.

Download English Version:

<https://daneshyari.com/en/article/1339927>

Download Persian Version:

<https://daneshyari.com/article/1339927>

[Daneshyari.com](https://daneshyari.com)